

Interaction between an Annular Crack and the Imperfect Interface in Magnetoelastic Layers

Yansong Li^{*}, Longjiang Bian, Jun Li

College of Civil Engineering, Hebei University of Engineering, Handan 056038, China

^{*}Corresponding author: liyshbue@163.com

Abstract The interaction between an annular crack and the interface is of practical significance. The interface, which is imperfect with the assumption that it is mechanically compliant and magnetoelastically weakly conducting. For a mechanically compliant interface tractions are continuous but displacements are discontinuous across the imperfect interface. For a magnetoelastically weakly conducting interface the normal electric displacement and magnetic induction are continuous but the electric and magnetic potentials are discontinuous across the interface. Such a problem is investigated by the method of singular integral equation in the present work. The field intensity factors and energy release rate are derived. Numerical results reveal the effects of electric or magnetic loadings, material parameters and interfacial imperfection on crack propagation and growth. The results seem useful for design of the magnetoelastic composite structures and devices of high performance.

Keywords Annular crack, Imperfect interface, Energy release rate, Magnetoelastic materials, Fracture mechanics

1. Introduction

Magnetoelastic materials, which are composed of a piezoelectric and piezomagnetic phase, not only have original piezoelectric and piezomagnetic properties but also exhibit a remarkable magneto-electric coupling effect that is not present in the constituents. Such composites have found increasing applications in several engineering fields such as magnetic field probes, electronic packaging, hydrophones, medical ultrasonic imaging and in general as transducers, sensors and actuators. Micromechanics modeling to predict and estimate the material properties of piezoelectric/piezomagnetic composites was presented [1-3].

These magnetoelastic materials are generally brittle; therefore cracks inevitably form during the manufacturing process and subsequent handling. For that reason, it is of great importance to study the fracture behavior of such composites and its influence on the coupled response. Recently, research on fracture mechanics of magnetoelastic materials has drawn increased interest. Most of the achievements are made on the anti-plane and in-plane crack problem [4-8]. For the axisymmetric crack in magnetoelastic materials, some progress has also been made. Studies related to penny-shaped or annular cracks can be found in the literature [9-11].

When two dissimilar materials bonded together, it is difficult to guarantee them to be perfectly bonded. Some interfacial models, i.e. spring-like model, are presented. Meguid and Wang [12] dealt with the interaction of crack and imperfect interface when dynamic antiplane shear waves are applied. a crack situated at the imperfect interface has been considered by Lenci [13], who found only the logarithmic stress singularity near the crack tips. Instead of the usual traction-free crack surface condition, Udea et al. [14] applied the spring-like imperfect interface condition to reconsider the corresponding antiplane shear problem, and found that the stress singularity at the crack tips is no longer an inverse square-root singularity, but a singularity of power law governed by the interface parameters. Zhong et al. [15] investigated the elastostatic problem of a mode-I crack embedded in a bimaterial with an imperfect interface.

This paper aims at analyzing the interaction of an annular crack and an imperfect interface. The interface, which is imperfect with the assumption that it is mechanically compliant and magnetoelectrically weakly conducting. For a mechanically compliant interface tractions are continuous but displacements are discontinuous across the imperfect interface. For a magnetoelectrically weakly conducting interface the normal electric displacement and magnetic induction are continuous but the electric and magnetic potentials are discontinuous across the interface. Using the Hankel transform technique, the associated mixed-boundary value problem is reduced to a singular integral equation. Numerical results are presented. The influences of interfacial imperfection on energy release rates near the crack tips are analyzed in detail.

2. Formulation of the problem

As shown in Fig. 1, two dissimilar magnetoelastoelectric materials bonded with an imperfect interface. For convenience, they are marked with material I and material II, which occupy the region $-h_2 < z < h_1$ and region $h_1 < z < h_1 + h_3$ respectively. An annular crack with the outer radius b and inner radius a perpendicular to the poling axis is situated in the magnetoelastoelectric material I and occupies the region $a \leq r \leq b$, $z = 0$. And the crack width c is introduced with $c = b - a$.

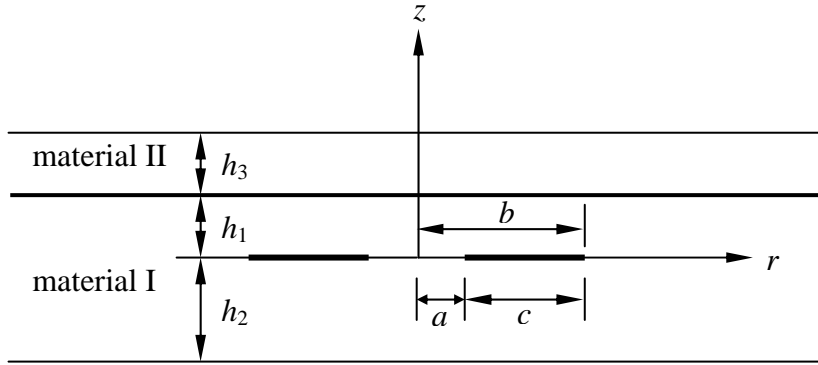


Figure 1. Configuration of the annular and imperfect interface in bonded magnetoelastoelectric layers

The boundary conditions for the magnetoelectrically impermeable annular crack and mechanically compliant and magnetoelectrically weakly conducting interface conditions are set as

$$\sigma_{rz}^{(1)}(r, 0) = \sigma_{rz}^{(2)}(r, 0) = p_1(r), \quad \sigma_{zz}^{(1)}(r, 0) = \sigma_{zz}^{(2)}(r, 0) = p_2(r), \quad (a < r < b) \quad (1)$$

$$D_{zj}^{(1)}(r, 0) = D_{zj}^{(2)}(r, 0) = p_3(r), \quad B_{zj}^{(1)}(r, 0) = B_{zj}^{(2)}(r, 0) = p_4(r), \quad (a < r < b) \quad (2)$$

$$u_{rj}^{(1)}(r, 0) = u_{rj}^{(2)}(r, 0), \quad u_{zj}^{(1)}(r, 0) = u_{zj}^{(2)}(r, 0), \quad (0 \leq r \leq a, b \leq r < \infty) \quad (3)$$

$$\phi_i^{(1)}(r, 0) = \phi_i^{(2)}(r, 0), \quad \psi_i^{(1)}(r, 0) = \psi_i^{(2)}(r, 0), \quad (0 \leq r \leq a, b \leq r < \infty) \quad (4)$$

$$\sigma_{rz}^{(1)}(r, 0) = \sigma_{rz}^{(2)}(r, 0), \quad \sigma_{zz}^{(1)}(r, 0) = \sigma_{zz}^{(2)}(r, 0), \quad (0 \leq r \leq a, b \leq r < \infty) \quad (5)$$

$$D_{zj}^{(1)}(r, 0) = D_{zj}^{(2)}(r, 0), \quad B_{zj}^{(1)}(r, 0) = B_{zj}^{(2)}(r, 0), \quad (0 \leq r \leq a, b \leq r < \infty) \quad (6)$$

$$\sigma_{rz}^{(2)}(r, -h_2) = 0, \quad \sigma_{zz}^{(2)}(r, -h_2) = 0, \quad D_{zj}^{(2)}(r, -h_2) = 0, \quad B_{zj}^{(2)}(r, -h_2) = 0 \quad (0 \leq r < \infty) \quad (7)$$

$$\sigma_{rz}^{(1)}(r, h_1) = \sigma_{rzII}(r, h_1), \quad \sigma_{zz}^{(1)}(r, h_1) = \sigma_{zzII}(r, h_1), \quad (8)$$

$$D_{zj}^{(1)}(r, h_1) = D_{zjII}(r, h_1), \quad B_{zj}^{(1)}(r, h_1) = B_{zjII}(r, h_1), \quad (0 \leq r < \infty) \quad (9)$$

$$u_{rj}^{(1)}(r, h_1) - u_{rjII}(r, h_1) = \beta_1 \sigma_{rzII}(r, h_1), \quad u_{zj}^{(1)}(r, h_1) - u_{zjII}(r, h_1) = \beta_2 \sigma_{zzII}(r, h_1), \quad (10)$$

$$\phi_{rI}^{(1)}(r, h_1) - \phi_{rII}(r, h_1) = \beta_3 D_{zII}(r, h_1), \psi_{rI}^{(1)}(r, h_1) - \psi_{rII}(r, h_1) = \beta_4 B_{zII}(r, h_1), (0 \leq r < \infty) \quad (11)$$

$$\sigma_{rzII}(r, h_1 + h_3) = 0, \sigma_{zzII}(r, h_1 + h_3) = 0, D_{zII}(r, h_1 + h_3) = 0, B_{zII}(r, h_1 + h_3) = 0 (0 \leq r < \infty) \quad (12)$$

where the superscripts (1) and (2) denote the upper and lower of the magnetoelastic material I, respectively; $p_1(r)$, $p_2(r)$, $p_3(r)$ and $p_4(r)$ are the given amplitude of the applied loadings. β_1 , β_2 , β_3 and β_4 are interface parameters, respectively.

For the axisymmetric problem, the government equations of magnetoelastic material are

$$c_{11} \left(\frac{\partial^2 u_r}{\partial r^2} + \frac{1}{r} \frac{\partial u_r}{\partial r} - \frac{1}{r^2} \right) + c_{44} \frac{\partial^2 u_r}{\partial z^2} + (c_{13} + c_{44}) \frac{\partial^2 u_z}{\partial r \partial z} + (e_{31} + e_{15}) \frac{\partial^2 \phi}{\partial r \partial z} + (f_{31} + f_{15}) \frac{\partial^2 \psi}{\partial r \partial z} = 0, \quad (13)$$

$$(c_{13} + c_{44}) \left(\frac{\partial^2 u_r}{\partial r \partial z} + \frac{1}{r} \frac{\partial u_r}{\partial z} \right) + c_{44} \left(\frac{\partial^2 u_z}{\partial r^2} + \frac{1}{r} \frac{\partial u_z}{\partial r} \right) + c_{33} \frac{\partial^2 u_z}{\partial z^2} + e_{15} \left(\frac{\partial^2 \phi}{\partial r^2} + \frac{1}{r} \frac{\partial \phi}{\partial r} \right) + e_{33} \frac{\partial^2 \phi}{\partial z^2} + f_{15} \left(\frac{\partial^2 \psi}{\partial r^2} + \frac{1}{r} \frac{\partial \psi}{\partial r} \right) + f_{33} \frac{\partial^2 \psi}{\partial z^2} = 0, \quad (14)$$

$$(e_{15} + e_{31}) \left(\frac{\partial^2 u_r}{\partial r \partial z} + \frac{1}{r} \frac{\partial u_r}{\partial z} \right) + e_{15} \left(\frac{\partial^2 u_z}{\partial r^2} + \frac{1}{r} \frac{\partial u_z}{\partial r} \right) + e_{33} \frac{\partial^2 u_z}{\partial z^2} - \varepsilon_{11} \left(\frac{\partial^2 \phi}{\partial r^2} + \frac{1}{r} \frac{\partial \phi}{\partial r} \right) - \varepsilon_{33} \frac{\partial^2 \phi}{\partial z^2} - g_{11} \left(\frac{\partial^2 \psi}{\partial r^2} + \frac{1}{r} \frac{\partial \psi}{\partial r} \right) - g_{33} \frac{\partial^2 \psi}{\partial z^2} = 0, \quad (15)$$

$$(f_{15} + f_{31}) \left(\frac{\partial^2 u_r}{\partial r \partial z} + \frac{1}{r} \frac{\partial u_r}{\partial z} \right) + f_{15} \left(\frac{\partial^2 u_z}{\partial r^2} + \frac{1}{r} \frac{\partial u_z}{\partial r} \right) + f_{33} \frac{\partial^2 u_z}{\partial z^2} - g_{11} \left(\frac{\partial^2 \phi}{\partial r^2} + \frac{1}{r} \frac{\partial \phi}{\partial r} \right) - g_{33} \frac{\partial^2 \phi}{\partial z^2} - \mu_{11} \left(\frac{\partial^2 \psi}{\partial r^2} + \frac{1}{r} \frac{\partial \psi}{\partial r} \right) - \mu_{33} \frac{\partial^2 \psi}{\partial z^2} = 0, \quad (16)$$

The generally solutions of the equations above mentioned are

$$u_r(r, z) = \sum_{j=1}^8 \int_0^\infty a_{1j} \exp(\rho \lambda_j z) A_j(\rho) J_1(\rho r) d\rho, \quad (17)$$

$$u_z(r, z) = \sum_{j=1}^8 \int_0^\infty a_{2j} \exp(\rho \lambda_j z) A_j(\rho) J_0(\rho r) d\rho, \quad (18)$$

$$\phi(r, z) = \sum_{j=1}^8 \int_0^\infty a_{3j} \exp(\rho \lambda_j z) A_j(\rho) J_0(\rho r) d\rho, \quad (19)$$

$$\psi(r, z) = \sum_{j=1}^8 \int_0^\infty a_{4j} \exp(\rho \lambda_j z) A_j(\rho) J_0(\rho r) d\rho, \quad (20)$$

where $A_j(\rho)$ ($j=1, 2, L, 8$) are unknown functions to be determined and J_i ($i=0, 1$) are i th order Bessel functions of the first kind. The constants $\{a_{1j}, a_{2j}, a_{3j}\}$ and parameters λ_j are constant related to material parameters.

3. The derivation of the integral equations

A set of new unknown functions are now introduced

$$d_1(r) = \frac{1}{r} \frac{\partial}{\partial r} \{ r u_{rI}^{(1)}(r, 0) - r u_{rI}^{(2)}(r, 0) \}, \quad (21)$$

$$d_2(r) = \frac{\partial}{\partial r} \left\{ u_{zr}^{(1)}(r, 0) - u_{zr}^{(2)}(r, 0) \right\}, \quad (22)$$

$$d_3(r) = \frac{\partial}{\partial r} \left\{ \phi_I^{(1)}(r, 0) - \phi_I^{(2)}(r, 0) \right\}, \quad (23)$$

$$d_4(r) = \frac{\partial}{\partial r} \left\{ \psi_I^{(1)}(r, 0) - \psi_I^{(2)}(r, 0) \right\}. \quad (24)$$

In the annular crack shown in Fig. 1, physical considerations require that

$$\left[u_r^{(1)}(r, 0) - u_r^{(2)}(r, 0) \right] \rightarrow 0, \text{ for } r \rightarrow a, b, \quad (25)$$

$$\left[u_z^{(1)}(r, 0) - u_z^{(2)}(r, 0) \right] \rightarrow 0, \text{ for } r \rightarrow a, b, \quad (26)$$

$$\left[\phi_I^{(1)}(r, 0) - \phi_I^{(2)}(r, 0) \right] \rightarrow 0 \text{ for } r \rightarrow a, b. \quad (27)$$

$$\left[\psi_I^{(1)}(r, 0) - \psi_I^{(2)}(r, 0) \right] \rightarrow 0 \text{ for } r \rightarrow a, b. \quad (28)$$

Therefore, the unknown function defined by Eq. (10) must satisfy the following conditions

$$\int_a^b r d_1(r) dr = 0, \quad (29)$$

$$\int_a^b d_2(r) dr = 0, \quad (30)$$

$$\int_a^b d_3(r) dr = 0, \quad (31)$$

$$\int_a^b d_4(r) dr = 0. \quad (32)$$

Substitute Eqs. (17)-(20) into boundary conditions Eqs. (1)-(12) and using Eqs. (21)-(24), one obtains

$$\frac{1}{\pi} \mathbf{M} \int_a^b \frac{1}{s-r} \mathbf{F}(s) ds + \frac{1}{\pi} \int_a^b \mathbf{Q} \mathbf{F}(s) ds = \mathbf{\Gamma}(r), \quad (33)$$

where

$$\mathbf{M} = \begin{bmatrix} M_{11} & 0 & 0 & 0 \\ 0 & M_{22} & M_{23} & M_{24} \\ 0 & M_{32} & M_{33} & M_{34} \\ 0 & M_{42} & M_{43} & M_{44} \end{bmatrix}, \quad (34)$$

$$\mathbf{Q} = \kappa \mathbf{M} + \pi \int_0^\infty \rho s \mathbf{J}_{10}(\rho r) [\mathbf{K}(\rho) - \mathbf{M}] \mathbf{J}_{01}(\rho s) d\rho, \quad (35)$$

$$M_{ij} = \lim_{\rho \rightarrow \infty} K_{ij}(\rho), \quad (36)$$

with $K_{ij}(\rho)$ can be found in Appendix A. And

$$\kappa = \text{diag} \left[\kappa_{11}(r, s), \kappa_{22}(r, s), \kappa_{22}(r, s), \kappa_{22}(r, s) \right], \quad (37)$$

$$\kappa_{11}(r, s) = \left[\frac{2rM_1(r, s)}{s^2 - r^2} - \frac{1}{s-r} \right], \quad (38)$$

$$\kappa_{22}(r, s) = \left[\frac{2sM_2(r, s)}{s^2 - r^2} - \frac{1}{s-r} \right], \quad (39)$$

and

$$M_1(r, s) = \begin{cases} \frac{s}{r} E(s/r), & s < r, \\ \frac{s^2}{r^2} E(r/s) - \frac{s^2 - r^2}{r^2} K(r/s), & s > r, \end{cases} \quad (40)$$

$$M_2(r, s) = \begin{cases} \frac{r}{s} E(s/r) + \frac{s^2 - r^2}{rs} K(s/r), & s < r, \\ E(r/s), & s > r. \end{cases} \quad (41)$$

Introducing two non-dimensional variables η and ξ

$$s = (b-a)\eta/2 + (b+a)/2, \quad (42)$$

$$r = (b-a)\xi/2 + (b+a)/2. \quad (43)$$

Eq. (33) becomes

$$\frac{\mathbf{M}}{\pi} \int_{-1}^1 \frac{\mathbf{G}(\eta)}{\eta - \xi} d\eta + \frac{1}{\pi} \int_{-1}^1 \bar{\mathbf{Q}}(\xi, \eta) \mathbf{G}(\eta) d\eta = \mathbf{L}(\xi), \quad (44)$$

where

$$\mathbf{G}(\eta) = \mathbf{F} \left(\frac{b-a}{2} \eta + \frac{b+a}{2} \right), \quad (45)$$

$$\bar{\mathbf{Q}}(\eta, \xi) = \frac{b-a}{2} \mathbf{Q} \left(\frac{b-a}{2} \eta + \frac{b+a}{2}, \frac{b-a}{2} \xi + \frac{b+a}{2} \right), \quad (46)$$

$$\mathbf{L}(\xi) = \Gamma \left(\frac{b-a}{2} \xi + \frac{b+a}{2} \right). \quad (47)$$

4. The solution of integral equations

So far, the Cauchy singular integral Eq. (44) and the single-valued conditions Eqs. (29)-(32) have been derived. By using the numerical method of Erdogan and Gupta [16], a system of linear algebraic equations can be obtained

$$\frac{1}{n} \sum_{l=1}^n \left(\frac{\mathbf{M}}{\eta_l - \xi_m} + \bar{\mathbf{Q}}(\eta_l, \xi_m) \right) \mathbf{R}(\eta_l) = \mathbf{L}(\xi_m), \quad (48)$$

$$\frac{1}{n} \sum_{l=1}^n \text{diag} \left(\left(\frac{b-a}{2} \right) \eta_l + \frac{b+a}{2}, 1, 1, 1 \right) \mathbf{R}(\eta_l) = 0, \quad (49)$$

where $\mathbf{R}(\eta) = \sqrt{1-\eta^2} \mathbf{G}(\eta)$, and n is the number of the discrete points of $\mathbf{R}(\eta_l)$ between -1 and $+1$. The discrete values of ξ_m and η_l are the roots of the Chebyshev polynomials of the first and second kind, respectively:

$$\xi_m = \cos(m\pi/n), \quad m = 1, 2, \dots, n-1, \quad (50)$$

$$\eta_l = \cos[(2l-1)\pi/2n], \quad l = 1, 2, \dots, n. \quad (51)$$

One may solve Eqs. (48) and (49) numerically to get the solutions of $\mathbf{R}(\eta_l)$, which can be further used to determine the stress intensity factor (SIF).

5. Field intensity factors and energy release rates

The field intensity factors (FIFs) including mode-I and mode-II stress intensity factors (SIFs) and electric displacement intensity factor (EDIF), which characterize magnitudes of stress, electric displacement respectively, of the outer and inner crack tips can be deduced

$$\mathbf{K}_b = \{K_{Ib} \quad K_{IIb} \quad K_{Db} \quad K_{Bb}\}^T = -\sqrt{\pi(b-a)/2\mathbf{MR}}(1) \quad (52)$$

and

$$\mathbf{K}_a = \{K_{Ia} \quad K_{IIa} \quad K_{Da} \quad K_{Ba}\}^T = \sqrt{\pi(b-a)/2\mathbf{MR}}(-1) \quad (53)$$

The energy release rates (ERRs) of the outer and inner crack tips can be derived as

$$G_v = \frac{1}{4} \mathbf{K}_v^T \mathbf{M}^{-1} \mathbf{K}_v, \quad (v = b, a) \quad (54)$$

6. Numerical results

For the numerical examples, magnetoelastic composite $\text{BaTiO}_3\text{-CoFe}_2\text{O}_4$ are used as materials I and II. For simplicity, only the loading case of $\Gamma(r) = \{0 \quad -\sigma_0 \quad -D_0 \quad -B_0\}^T$ is considered. Also, D_0 and B_0 are determined by the load combination parameters $\lambda_D = D_0 c_{33} / (\sigma_0 e_{33})$ and $\lambda_B = D_0 c_{33} / (\sigma_0 f_{33})$. The numerical results are plotted in Figs. 2-5, where ERRs, G_b and G_a , are normalized by G_0 , which can be expressed as

$$G_0 = \frac{\pi}{8} \Lambda_{22} \sigma_0^2 c, \quad (55)$$

where Λ_{22} is the element of matrix Λ , and

$$\Lambda = \mathbf{M}^{-1}. \quad (56)$$

Figs. 2 and 3 show the effects of β_1 and β_2 on the normalized ERRs of the outer and inner crack-tips. From Fig. 2, it is clear that the normalized ERRs increase with increasing β_1 . Similar phenomena can be observe in Fig. 3. This means that increasing β_1 and β_2 will promote the crack propagation or growth.

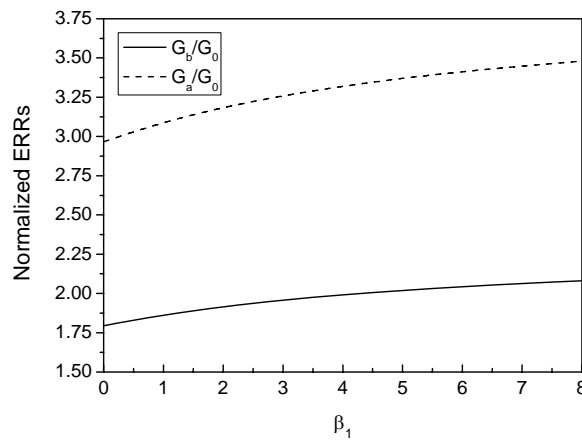


Figure 2. The effect of β_1 on the normalized ERRs of the outer and inner crack tips of an annular crack

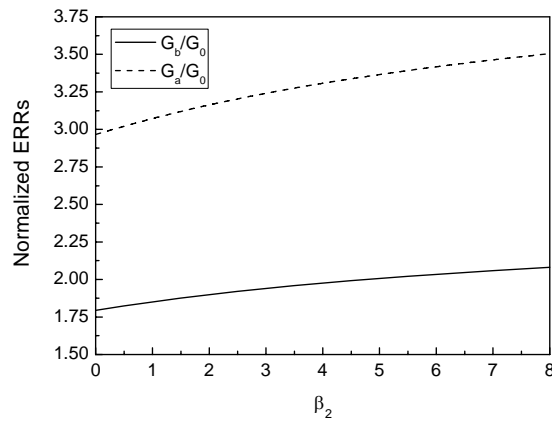


Figure 3. The effect of β_2 on the normalized ERRs of the outer and inner crack tips of an annular crack

The effects of β_3 and β_4 on the normalized ERRs are plotted in Figs. 4 and 5. From these figures, one knows that the normalized ERRs are almost independence of β_3 and β_4 .

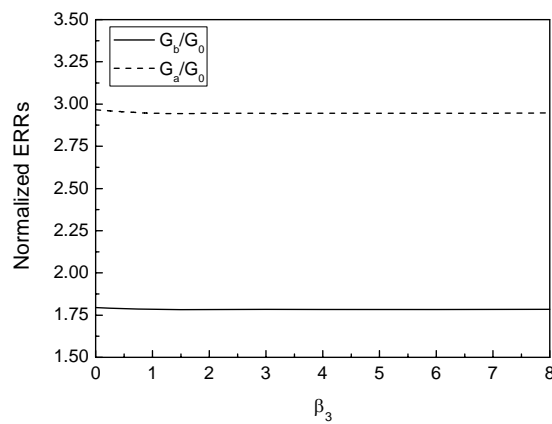


Figure 4. The effect of β_3 on the normalized ERRs of the outer and inner crack tips of an annular crack

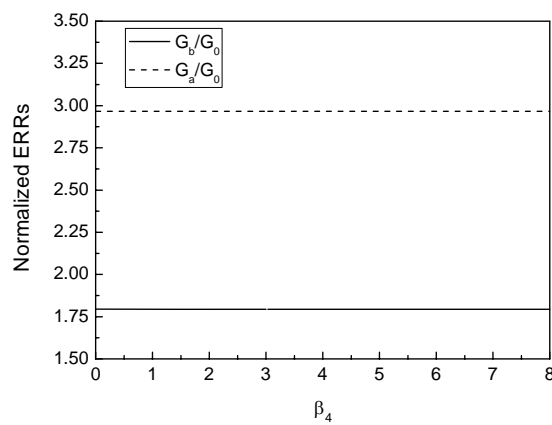


Figure 5. The effect of β_4 on the normalized ERRs of the outer and inner crack tips of an annular crack

From Figs. 2-5, one can also know that the fracture parameters ERR of the inner crack tip of the annular crack are always larger than those of the outer one.

7. Conclusions

In this paper, the interaction of an annular crack and an imperfect interface in bonded magneto-electroelastic layers is investigated. The interface, which is imperfect with the assumption that it is mechanically compliant and magnetoelectrically weakly conducting. Using the Hankel transform technique, the associated mixed-boundary value problem is reduced to a singular integral equation, which are further reduced to a system of algebraic equations. Finally, the field intensity factor and energy release rate are determined and numerically solved. The following conclusions may be drawn:

- (i) Different interfacial parameters have different influences on the propagation and growth of the annular crack. Increasing β_1 and β_2 can promote the crack propagation or growth. However, the effects of β_3 and β_4 on energy release rates are very small.
- (ii) The energy release rates of the inner crack tip of the annular crack are always larger than those of the outer one.

Appendix A

The matrix $\mathbf{K}(\rho)$ can be expressed as

$$\mathbf{K}(\rho) = \frac{1}{\rho} \begin{bmatrix} \sum_{j=1}^8 \frac{H_{17j} \Delta_{21j}(\rho)}{\Delta(\rho)} & -\sum_{j=1}^8 \frac{H_{17j} \Delta_{22j}(\rho)}{\Delta(\rho)} & -\sum_{j=1}^8 \frac{H_{17j} \Delta_{23j}(\rho)}{\Delta(\rho)} & -\sum_{j=1}^8 \frac{H_{17j} \Delta_{24j}(\rho)}{\Delta(\rho)} \\ \sum_{j=1}^8 \frac{H_{18j} \Delta_{21j}(\rho)}{\Delta(\rho)} & -\sum_{j=1}^8 \frac{H_{18j} \Delta_{22j}(\rho)}{\Delta(\rho)} & -\sum_{j=1}^8 \frac{H_{18j} \Delta_{23j}(\rho)}{\Delta(\rho)} & -\sum_{j=1}^8 \frac{H_{18j} \Delta_{24j}(\rho)}{\Delta(\rho)} \\ \sum_{j=1}^8 \frac{H_{19j} \Delta_{21j}(\rho)}{\Delta(\rho)} & \sum_{j=1}^8 \frac{H_{19j} \Delta_{22j}(\rho)}{\Delta(\rho)} & \sum_{j=1}^8 \frac{H_{19j} \Delta_{23j}(\rho)}{\Delta(\rho)} & \sum_{j=1}^8 \frac{H_{19j} \Delta_{24j}(\rho)}{\Delta(\rho)} \\ \sum_{j=1}^8 \frac{H_{20j} \Delta_{21j}(\rho)}{\Delta(\rho)} & \sum_{j=1}^8 \frac{H_{20j} \Delta_{22j}(\rho)}{\Delta(\rho)} & \sum_{j=1}^8 \frac{H_{20j} \Delta_{23j}(\rho)}{\Delta(\rho)} & \sum_{j=1}^8 \frac{H_{20j} \Delta_{24j}(\rho)}{\Delta(\rho)} \end{bmatrix},$$

where $\Delta(\rho)$ is the determinant of the coefficient matrix \mathbf{H} , whose elements can be expressed as H_{ij} with i th row and j th column; $\Delta_{kj}(\rho)$ ($k = 21, 22, 23, 24$) are, respectively, the corresponding algebra cofactors. The components of \mathbf{H} are given by

$$\begin{aligned} H_{1j} &= (c_{44II} \lambda_{jII} a_{1jII} - c_{44II} a_{2jII} - e_{15II} a_{3jII} - f_{15II} a_{4jII}) \exp(\rho \lambda_{jII} (h_1 + h_3)), H_{1(j+8)} = 0, H_{1(j+16)} = 0, \\ H_{2j} &= (c_{13II} a_{1jII} + c_{33II} \lambda_{jII} a_{2jII} + e_{33II} \lambda_{jII} a_{3jII} + f_{33II} \lambda_{jII} a_{4jII}) \exp(\rho \lambda_{jII} (h_1 + h_3)), H_{2(j+8)} = 0, H_{2(j+16)} = 0, \\ H_{3j} &= (e_{31II} a_{1jII} + e_{33II} \lambda_{jII} a_{2jII} - \varepsilon_{33II} \lambda_{jII} a_{3jII} - g_{33II} \lambda_{jII} a_{4jII}) \exp(\rho \lambda_{jII} (h_1 + h_3)), H_{3(j+8)} = 0, H_{3(j+16)} = 0, \\ H_{4j} &= (f_{31II} a_{1jII} + f_{33II} \lambda_{jII} a_{2jII} - g_{33II} \lambda_{jII} a_{3jII} - \mu_{33II} \lambda_{jII} a_{4jII}) \exp(\rho \lambda_{jII} (h_1 + h_3)), H_{4(j+8)} = 0, H_{4(j+16)} = 0, \\ H_{5j} &= 0, H_{5(j+8)} = 0, H_{5(j+16)} = (c_{44I} \lambda_{jI} a_{1jI} - c_{44I} a_{2jI} - e_{15I} a_{3jI} - f_{15I} a_{4jI}) \exp(-\rho \lambda_{jI} h_2), \\ H_{6j} &= 0, H_{6(j+8)} = 0, H_{6(j+16)} = (c_{13I} a_{1jI} + c_{33I} \lambda_{jI} a_{2jI} + e_{33I} \lambda_{jI} a_{3jI} + f_{33I} \lambda_{jI} a_{4jI}) \exp(-\rho \lambda_{jI} h_2), \end{aligned}$$

$$\begin{aligned}
H_{7j} &= 0, H_{7(j+8)} = 0, H_{7(j+16)} = \left(e_{31I} a_{1jI} + e_{33I} \lambda_{jI} a_{2jI} - \varepsilon_{33I} \lambda_{jI} a_{3jI} - g_{33I} \lambda_{jI} a_{4jI} \right) \exp(-\rho \lambda_{jI} h_2), \\
H_{8j} &= 0, H_{8(j+8)} = 0, H_{8(j+16)} = \left(f_{31I} a_{1jI} + f_{33I} \lambda_{jI} a_{2jI} - g_{33I} \lambda_{jI} a_{3jI} - \mu_{33I} \lambda_{jI} a_{4jI} \right) \exp(-\rho \lambda_{jI} h_2), \\
H_{9j} &= \left(c_{44II} \lambda_{jII} a_{1jII} - c_{44II} a_{2jII} - e_{15II} a_{3jII} - f_{15II} a_{4jII} \right) \exp(\rho \lambda_{jII} h_1), \\
H_{9(j+8)} &= -\left(c_{44I} \lambda_{jI} a_{1jI} - c_{44I} a_{2jI} - e_{15I} a_{3jI} - f_{15I} a_{4jI} \right) \exp(\rho \lambda_{jI} h_1), H_{9(j+16)} = 0, \\
H_{10j} &= \left(c_{13II} a_{1jII} + c_{33II} \lambda_{jII} a_{2jII} + e_{33II} \lambda_{jII} a_{3jII} + f_{33II} \lambda_{jII} a_{4jII} \right) \exp(\rho \lambda_{jII} h_1), \\
H_{10(j+8)} &= -\left(c_{13I} a_{1jI} + c_{33I} \lambda_{jI} a_{2jI} + e_{33I} \lambda_{jI} a_{3jI} + f_{33I} \lambda_{jI} a_{4jI} \right) \exp(\rho \lambda_{jI} h_1), H_{10(j+16)} = 0, \\
H_{11j} &= \left(e_{31II} a_{1jII} + e_{33II} \lambda_{jII} a_{2jII} - \varepsilon_{33II} \lambda_{jII} a_{3jII} - g_{33II} \lambda_{jII} a_{4jII} \right) \exp(\rho \lambda_{jII} h_1), \\
H_{11(j+8)} &= -\left(e_{31I} a_{1jI} + e_{33I} \lambda_{jI} a_{2jI} - \varepsilon_{33I} \lambda_{jI} a_{3jI} - g_{33I} \lambda_{jI} a_{4jI} \right) \exp(\rho \lambda_{jI} h_1), H_{11(j+16)} = 0, \\
H_{12j} &= \left(f_{31II} a_{1jII} + f_{33II} \lambda_{jII} a_{2jII} - g_{33II} \lambda_{jII} a_{3jII} - \mu_{33II} \lambda_{jII} a_{4jII} \right) \exp(\rho \lambda_{jII} h_1), \\
H_{12(j+8)} &= -\left(f_{31I} a_{1jI} + f_{33I} \lambda_{jI} a_{2jI} - g_{33I} \lambda_{jI} a_{3jI} - \mu_{33I} \lambda_{jI} a_{4jI} \right) \exp(\rho \lambda_{jI} h_1), H_{12(j+16)} = 0, \\
H_{13j} &= \left[a_{1jII} / \rho - \beta_1 \left(c_{44II} \lambda_{jII} a_{1jII} - c_{44II} a_{2jII} - e_{15II} a_{3jII} - f_{15II} a_{4jII} \right) \right] \exp(\rho \lambda_{jII} h_1), \\
H_{13(j+8)} &= -\left(a_{1jI} / \rho \right) \exp(\rho \lambda_{jI} h_1), H_{13(j+16)} = 0, \\
H_{14j} &= \left[a_{2jII} / \rho - \beta_2 \left(c_{13II} a_{1jII} + c_{33II} \lambda_{jII} a_{2jII} + e_{33II} \lambda_{jII} a_{3jII} + f_{33II} \lambda_{jII} a_{4jII} \right) \right] \exp(\rho \lambda_{jII} h_1), \\
H_{14(j+8)} &= -\left(a_{2jI} / \rho \right) \exp(\rho \lambda_{jI} h_1), H_{14(j+16)} = 0, \\
H_{15j} &= \left[a_{3jII} / \rho - \beta_3 \left(e_{31II} a_{1jII} + e_{33II} \lambda_{jII} a_{2jII} - \varepsilon_{33II} \lambda_{jII} a_{3jII} - g_{33II} \lambda_{jII} a_{4jII} \right) \right] \exp(\rho \lambda_{jII} h_1), \\
H_{15(j+8)} &= -\left(a_{3jI} / \rho \right) \exp(\rho \lambda_{jI} h_1), H_{15(j+16)} = 0, \\
H_{16j} &= \left[a_{4jII} / \rho - \beta_4 \left(f_{31II} a_{1jII} + f_{33II} \lambda_{jII} a_{2jII} - g_{33II} \lambda_{jII} a_{3jII} - \mu_{33II} \lambda_{jII} a_{4jII} \right) \right] \exp(\rho \lambda_{jII} h_1), \\
H_{16(j+8)} &= -\left(a_{4jI} / \rho \right) \exp(\rho \lambda_{jI} h_1), H_{16(j+16)} = 0, \\
H_{17j} &= 0, H_{17(j+8)} = \left(c_{44I} \lambda_{jI} a_{1jI} - c_{44I} a_{2jI} - e_{15I} a_{3jI} - f_{15I} a_{4jI} \right), \\
H_{17(j+16)} &= -\left(c_{44I} \lambda_{jI} a_{1jI} - c_{44I} a_{2jI} - e_{15I} a_{3jI} - f_{15I} a_{4jI} \right), \\
H_{18j} &= 0, H_{18(j+8)} = \left(c_{13I} a_{1jI} + c_{33I} \lambda_{jI} a_{2jI} + e_{33I} \lambda_{jI} a_{3jI} + f_{33I} \lambda_{jI} a_{4jI} \right), \\
H_{18(j+16)} &= -\left(c_{13I} a_{1jI} + c_{33I} \lambda_{jI} a_{2jI} + e_{33I} \lambda_{jI} a_{3jI} + f_{33I} \lambda_{jI} a_{4jI} \right), \\
H_{19j} &= 0, H_{19(j+8)} = \left(e_{31I} a_{1jI} + e_{33I} \lambda_{jI} a_{2jI} - \varepsilon_{33I} \lambda_{jI} a_{3jI} - g_{33I} \lambda_{jI} a_{4jI} \right), \\
H_{19(j+16)} &= -\left(e_{31I} a_{1jI} + e_{33I} \lambda_{jI} a_{2jI} - \varepsilon_{33I} \lambda_{jI} a_{3jI} - g_{33I} \lambda_{jI} a_{4jI} \right), \\
H_{20j} &= 0, H_{20(j+8)} = \left(f_{31I} a_{1jI} + f_{33I} \lambda_{jI} a_{2jI} - g_{33I} \lambda_{jI} a_{3jI} - \mu_{33I} \lambda_{jI} a_{4jI} \right), \\
H_{20(j+16)} &= -\left(f_{31I} a_{1jI} + f_{33I} \lambda_{jI} a_{2jI} - g_{33I} \lambda_{jI} a_{3jI} - \mu_{33I} \lambda_{jI} a_{4jI} \right), \\
H_{21j} &= 0, H_{21(j+8)} = a_{1jI} / \rho, H_{21(j+16)} = -a_{1jI} / \rho, \\
H_{22j} &= 0, H_{22(j+8)} = a_{2jI} / \rho, H_{22(j+16)} = -a_{2jI} / \rho, \\
H_{23j} &= 0, H_{23(j+8)} = a_{3jI} / \rho, H_{23(j+16)} = -a_{3jI} / \rho, \\
H_{24j} &= 0, H_{24(j+8)} = a_{4jI} / \rho, H_{24(j+16)} = -a_{4jI} / \rho,
\end{aligned}$$

where $j = 1, 2, L, 8$.

Acknowledgements

The authors wish to acknowledge the support from the Natural Science Fund of China (11072160).

References

- [1] Y. Benveniste, Magnetolectric effect in fibrous composites with piezoelectric and piezomagnetic phases. *Phys Rev B*, 51 (1995) 16424–16427.
- [2] J. Aboudi, Micromechanical analysis of fully coupled electro-magneto-thermo-elastic multiphase composites. *Smart Mater Struct*, 10 (2001) 867–877.
- [3] S. Priya, R. Islam, S.X. Dong, D. Vohland, Recent advancements in magnetolectric particular and laminate composites. *J Electroceram*, 19 (2007) 149–66.
- [4] J.X. Liu, X.L. Liu, Y.M. Zhao, Green's functions for anisotropic magneto-electroelastic solids with an elliptical cavity or a crack. *Int J Eng Sci*, 39 (2001) 1405–1418.
- [5] C.F. Gao, H. Kessler, H. Balke, Crack problems in magneto-electroelastic solids. Part I: exact solution of a crack. *Int J Eng Sci*, 41 (2003) 969–981.
- [6] G.C. Sih, Z.F. Song, Piezomagnetic and piezoelectric poling effects on mode I and II crack initiation behaviour of magneto-electroelastic materials composite. *Theor Appl Fract Mech*, 40 (2003) 161–186.
- [7] B.L. Wang, Y.W. Mai, Applicability of the crack-face electromagnetic boundary conditions for fracture of magneto-electroelastic materials. *Int J Solids Struct*, 44 (2007) 387–398
- [8] X.F. Li, G.L. Liu, K.Y. Lee, Magneto-electroelastic field induced by a crack terminating at the interface of a bi-magneto-electric material. *Philo Mag*, 89 (2009) 449–463.
- [9] W.J. Feng, E. Pan, X. Wang, Dynamic fracture analysis of a penny-shaped crack in a magneto-electroelastic layer. *Int J Solids Struct*, 44 (2007) 7955–7974.
- [10] M.H. Zhao, F. Yang, T. Liu, Analysis of a penny-shaped crack in a magneto-electro-elastic medium. *Philo Mag*, 86 (2006) 4397–4416.
- [11] Y.S. Li, Y.Y. Jiang, J.H. Ren, Z.Y. Cai, An annular interfacial crack between dissimilar magneto-electroelastic layers. *Smart Mater Struct*, 20 (2011) 085011.
- [12] S.A. Meguid, X.D. Wang, Wave scattering from cracks and imperfectly bonded inhomogeneities in advanced materials. *Mech Mater*, 31 (1999) 187–195.
- [13] S. Lenci, Analysis of a crack at a weak interface. *Int J Fract*, 108 (2001) 275–298.
- [14] S. Ueda, S. Biwa, K. Watanabe, R. Heuer, C. Pecorari, On the stiffness of spring model for closed crack. *Int J Eng Sci*, 44 (2006) 874–888.
- [15] X.C. Zhong, X.F. Li, K.Y. Lee, Analysis of a mode-I crack perpendicular to an imperfect interface. *Int J Solids Struct*, 46 (2009) 1456–1463.
- [16] F. Erdogan, G.D. Gupta, On the numerical solution of singular integral equations. *Quart Appl Math*, 29 (1972) 525–539.